Letter

Study of the decay $D_s^+ \to \pi^+\pi^+\pi^-\eta$ and observation of the W-annihilation decay $D_s^+ \to a_0(980)^+\rho^0$

M. Ablikim,[1] M. N. Achasov,[10,c] P. Adlarson,[67] S. Ahmed,[15] M. Albrecht,[4] R. Aliberti,[28] A. Amoroso,[66a,66c] M. R. An,[32] Q. An,[63,49] X. H. Bai,[57] Y. Bai,[48] O. Bakina,[29] R. Baldini Ferroli,[23a] I. Balossino,[24a] Y. Ban,[38,k] K. Begzsuren,[26] N. Berger,[28] M. Bertani,[23a] D. Bettoni,[24a] F. Bianchi,[66a,66c] J. Bloms,[60] A. Bortone,[66a,66c] I. Boyko,[29] R. A. Briere,[5] H. Cai,[68] X. Cai,[1,49] A. Calcaterra,[23a] G. F. Cao,[1,54] N. Cao,[1,54] S. A. Cetin,[53a] J. F. Chang,[1,49] W. L. Chang,[1,54] G. Chelkov,[29,b] D. Y. Chen,[6] G. Chen,[1] H. S. Chen,[1,54] M. L. Chen,[1,49] S. J. Chen,[35] X. R. Chen,[25] Y. B. Chen,[1,49] Z. J. Chen,[20,l] W. S. Cheng,[66c] G. Cibinetto,[24a] F. Cossio,[66c] X. F. Cui,[36] H. L. Dai,[1,49] X. C. Dai,[1,54] A. Dbeyssi,[15] R. E. de Boer,[4] D. Dedovich,[29] Z. Y. Deng,[1] A. Denig,[28] I. Denysenko,[29] M. Destefanis,[66a,66c] F. De Mori,[66a,66c] Y. Ding,[33] C. Dong,[36] J. Dong,[1,49] L. Y. Dong,[1,54] M. Y. Dong,[1,49,54] X. Dong,[68] S. X. Du,[71] Y. L. Fan,[68] J. Fang,[1,49] S. S. Fang,[1,54] Y. Fang,[1] R. Farinelli,[24a] L. Fava,[66b,66c] F. Feldbauer,[4] G. Felici,[23a] C. Q. Feng,[63,49] J. H. Feng,[50] M. Fritsch,[4] C. D. Fu,[1] Y. Gao,[64] Y. Gao,[63,49] Y. Gao,[38,k] Y. G. Gao,[6] I. Garzia,[24a,24b] P. T. Ge,[68] C. Geng,[50] E. M. Gersabeck,[58] A. Gilman,[61] K. Goetzen,[11] L. Gong,[33] W. X. Gong,[1,49] W. Gradl,[28] M. Greco,[66a,66c] L. M. Gu,[35] M. H. Gu,[1,49] S. Gu,[2] Y. T. Gu,[13] C. Y. Guan,[1,54] A. Q. Guo,[22] L. B. Guo,[34] R. P. Guo,[40] Y. P. Guo,[9,h] A. Guskov,[29] T. T. Han,[41] W. Y. Han,[32] X. Q. Hao,[16] F. A. Harris,[56] N. Hüsken,[22,28] K. L. He,[1,54] F. H. Heinsius,[4] C. H. Heinz,[28] T. Held,[4] Y. K. Heng,[1,49,54] C. Herold,[51] M. Himmelreich,[11,f] T. Holtmann,[4] Y. R. Hou,[54] Z. L. Hou,[1] H. M. Hu,[1,54] J. F. Hu,[47,m] T. Hu,[1,49,54] Y. Hu,[1] G. S. Huang,[63,49] L. Q. Huang,[64] X. T. Huang,[41] Y. P. Huang,[1] Z. Huang,[38,k] T. Hussain,[65] W. Ikegami Andersson,[67] W. Imoehl,[22] M. Irshad,[63,49] S. Jaeger,[4] S. Janchiv,[26,j] Q. Ji,[1] Q. P. Ji,[16] X. B. Ji,[1,54] X. L. Ji,[1,49] H. B. Jiang,[41] X. S. Jiang,[1,49,54] J. B. Jiao,[41] Z. Jiao,[18] S. Jin,[35] Y. Jin,[57] T. Johansson,[67] N. Kalantar-Nayestanaki,[55] X. S. Kang,[33] R. Kappert,[55] M. Kavatsyuk,[55] B. C. Ke,[43,1] I. K. Keshk,[4] A. Khoukaz,[60] P. Kiese,[28] R. Kiuchi,[1] R. Kliemt,[11] L. Koch,[30] O. B. Kolcu,[53a,e] B. Kopf,[4] M. Kuemmel,[4] M. Kuessner,[4] A. Kupsc,[67] M. G. Kurth,[1,54] W. Kühn,[30] J. J. Lane,[58] J. S. Lange,[30] P. Larin,[15] A. Lavania,[21] L. Lavezzi,[66a,66c] Z. H. Lei,[63,49] H. Leithoff,[28] M. Lellmann,[28] T. Lenz,[28] C. Li,[39] C. H. Li,[32] Cheng Li,[63,49] D. M. Li,[71] F. Li,[1,49] G. Li,[1] H. Li,[43] H. Li,[63,49] H. B. Li,[1,54] H. J. Li,[9,h] J. L. Li,[41] J. Q. Li,[4] J. S. Li,[50] Ke Li,[1] L. K. Li,[1] Lei Li,[3] P. R. Li,[31] S. Y. Li,[52] W. D. Li,[1,54] W. G. Li,[1] X. H. Li,[63,49] X. L. Li,[41] Z. Y. Li,[50] H. Liang,[63,49] H. Liang,[1,54] H. Liang,[27] Y. F. Liang,[45] Y. T. Liang,[25] L. Z. Liao,[1,54] J. Libby,[21] C. X. Lin,[50] B. J. Liu,[1] C. X. Liu,[1] D. Liu,[63,49] F. H. Liu,[44] Fang Liu,[1] Feng Liu,[6] H. B. Liu,[13] H. M. Liu,[1,54] Huanhuan Liu,[1] Huihui Liu,[17] J. B. Liu,[63,49] J. L. Liu,[64] J. Y. Liu,[1,54] K. Liu,[1] K. Y. Liu,[33] Ke Liu,[6] L. Liu,[63,49] M. H. Liu,[9,h] P. L. Liu,[1] Q. Liu,[54] Q. Liu,[68] S. B. Liu,[63,49] Shuai Liu,[46] T. Liu,[1,54] W. M. Liu,[63,49] X. Liu,[31] Y. Liu,[31] Y. B. Liu,[36] Z. A. Liu,[1,49,54] Z. Q. Liu,[41] X. C. Lou,[1,49,54] F. X. Lu,[50] F. X. Lu,[16] H. J. Lu,[18] J. D. Lu,[1,54] J. G. Lu,[1,49] X. L. Lu,[1] Y. Lu,[1] Y. P. Lu,[1,49] C. L. Luo,[34] M. X. Luo,[70] P. W. Luo,[50] T. Luo,[9,h] X. L. Luo,[1,49] S. Lusso,[66c] X. R. Lyu,[54] F. C. Ma,[33] H. L. Ma,[1] L. L. Ma,[41] M. M. Ma,[1,54] Q. M. Ma,[1] R. Q. Ma,[1,54] R. T. Ma,[54] X. X. Ma,[1,54] X. Y. Ma,[1,49] F. E. Maas,[15] M. Maggiora,[66a,66c] S. Maldaner,[4] S. Malde,[61] A. Mangoni,[23b] Y. J. Mao,[38,k] Z. P. Mao,[1] S. Marcello,[66a,66c] Z. X. Meng,[57] J. G. Messchendorp,[55] G. Mezzadri,[24a] T. J. Min,[35] R. E. Mitchell,[22] X. H. Mo,[1,49,54] Y. J. Mo,[6] N. Yu. Muchnoi,[10,c] H. Muramatsu,[59] S. Nakhoul,[11,f] Y. Nefedov,[29] F. Nerling,[11,f] I. B. Nikolaev,[10,c] Z. Ning,[1,49] S. Nisar,[8,i] S. L. Olsen,[54] Q. Ouyang,[1,49,54] S. Pacetti,[23b,23c] X. Pan,[9,h] Y. Pan,[58] A. Pathak,[1] P. Patteri,[23a] M. Pelizaeus,[4] H. P. Peng,[63,49] K. Peters,[11,f] J. Pettersson,[67] J. L. Ping,[34] R. G. Ping,[1,54] R. Poling,[59] V. Prasad,[63,49] H. Qi,[63,49] H. R. Qi,[52] K. H. Qi,[25] M. Qi,[35] T. Y. Qi,[9] T. Y. Qi,[2] S. Qian,[1,49] W. B. Qian,[54] Z. Qian,[50] C. F. Qiao,[54] L. Q. Qin,[12] X. P. Qin,[9] X. S. Qin,[41] Z. H. Qin,[1,49] J. F. Qiu,[1] S. Q. Qu,[36] K. Ravindran,[21] C. F. Redmer,[28] A. Rivetti,[66c] V. Rodin,[55] M. Rolo,[66c] G. Rong,[1,54] Ch. Rosner,[15] M. Rump,[60] H. S. Sang,[63] A. Sarantsev,[29,d] Y. Schelhaas,[28] C. Schnier,[4] K. Schoenning,[67] M. Scodeggio,[24a,24b] D. C. Shan,[46] W. Shan,[19] X. Y. Shan,[63,49] J. F. Shangguan,[46] M. Shao,[63,49] C. P. Shen,[9] P. X. Shen,[36] X. Y. Shen,[1,54] H. C. Shi,[63,49] R. S. Shi,[1,54] X. Shi,[1,49] X. D. Shi,[63,49] J. J. Song,[41] W. M. Song,[27,1] Y. X. Song,[38,k] S. Sosio,[66a,66c] S. Spataro,[66a,66c] K. X. Su,[68] P. P. Su,[46] F. F. Sui,[41] G. X. Sun,[1] H. K. Sun,[1] J. F. Sun,[16] L. Sun,[68] S. S. Sun,[1,54] T. Sun,[1,54] W. Y. Sun,[34] W. Y. Sun,[27] X. Sun,[20,l] Y. J. Sun,[63,49] Y. K. Sun,[63,49] Y. Z. Sun,[1] Z. T. Sun,[1] Y. H. Tan,[68] Y. X. Tan,[63,49] C. J. Tang,[45] G. Y. Tang,[1] J. Tang,[50] J. X. Teng,[63,49] V. Thoren,[67] Y. T. Tian,[25] I. Uman,[53b] B. Wang,[1] C. W. Wang,[35] D. Y. Wang,[38,k] H. J. Wang,[31] H. P. Wang,[1,54] K. Wang,[1,49] L. L. Wang,[1] M. Wang,[41] M. Z. Wang,[38,k] Meng Wang,[1,54] W. Wang,[50] W. H. Wang,[68] W. P. Wang,[63,49] X. Wang,[38,k] X. F. Wang,[31] X. L. Wang,[9,h] Y. Wang,[63,49] Y. Wang,[50] Y. D. Wang,[37] Y. F. Wang,[1,49,54] Y. Q. Wang,[1] Y. Y. Wang,[31] Z. Wang,[1,49] Z. Y. Wang,[1] Ziyi Wang,[54] Zongyuan Wang,[1,54] D. H. Wei,[12] P. Weidenkaff,[28] F. Weidner,[60] S. P. Wen,[1] D. J. White,[58] U. Wiedner,[4] G. Wilkinson,[61] M. Wolke,[67] L. Wollenberg,[4] J. F. Wu,[1,54] L. H. Wu,[1] L. J. Wu,[1,54] X. Wu,[9,h] Z. Wu,[1,49] L. Xia,[63,49] H. Xiao,[9,h] S. Y. Xiao,[1] Z. J. Xiao,[34] X. H. Xie,[38,k] Y. G. Xie,[1,49] Y. H. Xie,[6] T. Y. Xing,[1,54] G. F. Xu,[1] Q. J. Xu,[14] W. Xu,[1,54] X. P. Xu,[46] Y. C. Xu,[54] F. Yan,[9,h] L. Yan,[9,h] W. B. Yan,[63,49] W. C. Yan,[71] Xu Yan,[46] H. J. Yang,[42,g] H. X. Yang,[1] L. Yang,[43] S. L. Yang,[54] Y. X. Yang,[12] Yifan Yang,[1,54] Zhi Yang,[25] M. Ye,[1,49] M. H. Ye,[7] J. H. Yin,[1] Z. Y. You,[50] B. X. Yu,[1,49,54] C. X. Yu,[36] G. Yu,[1,54] J. S. Yu,[20,l] T. Yu,[64] C. Z. Yuan,[1,54] L. Yuan,[2] X. Q. Yuan,[38,k] Y. Yuan,[1] Z. Y. Yuan,[50] C. X. Yue,[32] A. Yuncu,[53a,a] A. A. Zafar,[65] Y. Zeng,[20,l] B. X. Zhang,[1] Guangyi Zhang,[16] H. Zhang,[63]

H. H. Zhang,[50] H. H. Zhang,[27] H. Y. Zhang,[1,49] J. J. Zhang,[43] J. L. Zhang,[69] J. Q. Zhang,[34] J. W. Zhang,[1,49,54] J. Y. Zhang,[1] J. Z. Zhang,[1,54] Jianyu Zhang,[1,54] Jiawei Zhang,[1,54] L. M. Zhang,[52] L. Q. Zhang,[50] Lei Zhang,[35] S. Zhang,[50] S. F. Zhang,[35] Shulei Zhang,[20,l] X. D. Zhang,[37] X. Y. Zhang,[41] Y. Zhang,[61] Y. H. Zhang,[1,49] Y. T. Zhang,[63,49] Yan Zhang,[63,49] Yao Zhang,[1] Yi Zhang,[9,h] Z. H. Zhang,[6] Z. Y. Zhang,[68] G. Zhao,[1] J. Zhao,[32] J. Y. Zhao,[1,54] J. Z. Zhao,[1,49] Lei Zhao,[63,49] Ling Zhao,[1] M. G. Zhao,[36] Q. Zhao,[1] S. J. Zhao,[71] Y. B. Zhao,[1,49] Y. X. Zhao,[25] Z. G. Zhao,[63,49] A. Zhemchugov,[29,b] B. Zheng,[64] J. P. Zheng,[1,49] Y. Zheng,[38,k] Y. H. Zheng,[54] B. Zhong,[34] C. Zhong,[64] L. P. Zhou,[1,54] Q. Zhou,[1,54] X. Zhou,[68] X. K. Zhou,[54] X. R. Zhou,[63,49] A. N. Zhu,[1,54] J. Zhu,[36] K. Zhu,[1] K. J. Zhu,[1,49,54] S. H. Zhu,[62] T. J. Zhu,[69] W. J. Zhu,[9,h] W. J. Zhu,[36] Y. C. Zhu,[63,49] Z. A. Zhu,[1,54] B. S. Zou,[1] and J. H. Zou[1]

(BESIII Collaboration)

[1]*Institute of High Energy Physics, Beijing 100049, People's Republic of China*
[2]*Beihang University, Beijing 100191, People's Republic of China*
[3]*Beijing Institute of Petrochemical Technology, Beijing 102617, People's Republic of China*
[4]*Bochum Ruhr-University, D-44780 Bochum, Germany*
[5]*Carnegie Mellon University, Pittsburgh, Pennsylvania 15213, USA*
[6]*Central China Normal University, Wuhan 430079, People's Republic of China*
[7]*China Center of Advanced Science and Technology, Beijing 100190, People's Republic of China*
[8]*COMSATS University Islamabad, Lahore Campus, Defence Road, Off Raiwind Road, 54000 Lahore, Pakistan*
[9]*Fudan University, Shanghai 200443, People's Republic of China*
[10]*G.I. Budker Institute of Nuclear Physics SB RAS (BINP), Novosibirsk 630090, Russia*
[11]*GSI Helmholtzcentre for Heavy Ion Research GmbH, D-64291 Darmstadt, Germany*
[12]*Guangxi Normal University, Guilin 541004, People's Republic of China*
[13]*Guangxi University, Nanning 530004, People's Republic of China*
[14]*Hangzhou Normal University, Hangzhou 310036, People's Republic of China*
[15]*Helmholtz Institute Mainz, Johann-Joachim-Becher-Weg 45, D-55099 Mainz, Germany*
[16]*Henan Normal University, Xinxiang 453007, People's Republic of China*
[17]*Henan University of Science and Technology, Luoyang 471003, People's Republic of China*
[18]*Huangshan College, Huangshan 245000, People's Republic of China*
[19]*Hunan Normal University, Changsha 410081, People's Republic of China*
[20]*Hunan University, Changsha 410082, People's Republic of China*
[21]*Indian Institute of Technology Madras, Chennai 600036, India*
[22]*Indiana University, Bloomington, Indiana 47405, USA*
[23a]*INFN Laboratori Nazionali di Frascati, I-00044 Frascati, Italy*
[23b]*INFN Sezione di Perugia, I-06100 Perugia, Italy*
[23c]*University of Perugia, I-06100 Perugia, Italy*
[24a]*INFN Sezione di Ferrara, I-44122 Ferrara, Italy*
[24b]*University of Ferrara, I-44122 Ferrara, Italy*
[25]*Institute of Modern Physics, Lanzhou 730000, People's Republic of China*
[26]*Institute of Physics and Technology, Peace Avenue 54B, Ulaanbaatar 13330, Mongolia*
[27]*Jilin University, Changchun 130012, People's Republic of China*
[28]*Johannes Gutenberg University of Mainz, Johann-Joachim-Becher-Weg 45, D-55099 Mainz, Germany*
[29]*Joint Institute for Nuclear Research, 141980 Dubna, Moscow region, Russia*
[30]*Justus-Liebig-Universitaet Giessen, II. Physikalisches Institut, Heinrich-Buff-Ring 16, D-35392 Giessen, Germany*
[31]*Lanzhou University, Lanzhou 730000, People's Republic of China*
[32]*Liaoning Normal University, Dalian 116029, People's Republic of China*
[33]*Liaoning University, Shenyang 110036, People's Republic of China*
[34]*Nanjing Normal University, Nanjing 210023, People's Republic of China*
[35]*Nanjing University, Nanjing 210093, People's Republic of China*
[36]*Nankai University, Tianjin 300071, People's Republic of China*
[37]*North China Electric Power University, Beijing 102206, People's Republic of China*
[38]*Peking University, Beijing 100871, People's Republic of China*
[39]*Qufu Normal University, Qufu 273165, People's Republic of China*
[40]*Shandong Normal University, Jinan 250014, People's Republic of China*
[41]*Shandong University, Jinan 250100, People's Republic of China*
[42]*Shanghai Jiao Tong University, Shanghai 200240, People's Republic of China*
[43]*Shanxi Normal University, Linfen 041004, People's Republic of China*

[44]*Shanxi University, Taiyuan 030006, People's Republic of China*
[45]*Sichuan University, Chengdu 610064, People's Republic of China*
[46]*Soochow University, Suzhou 215006, People's Republic of China*
[47]*South China Normal University, Guangzhou 510006, People's Republic of China*
[48]*Southeast University, Nanjing 211100, People's Republic of China*
[49]*State Key Laboratory of Particle Detection and Electronics, Beijing 100049, Hefei 230026, People's Republic of China*
[50]*Sun Yat-Sen University, Guangzhou 510275, People's Republic of China*
[51]*Suranaree University of Technology, University Avenue 111, Nakhon Ratchasima 30000, Thailand*
[52]*Tsinghua University, Beijing 100084, People's Republic of China*
[53a]*Turkish Accelerator Center Particle Factory Group, Istanbul Bilgi University, 34060 Eyup, Istanbul, Turkey*
[53b]*Near East University, Nicosia, North Cyprus, Mersin 10, Turkey*
[54]*University of Chinese Academy of Sciences, Beijing 100049, People's Republic of China*
[55]*University of Groningen, NL-9747 AA Groningen, Netherlands*
[56]*University of Hawaii, Honolulu, Hawaii 96822, USA*
[57]*University of Jinan, Jinan 250022, People's Republic of China*
[58]*University of Manchester, Oxford Road, Manchester M13 9PL, United Kingdom*
[59]*University of Minnesota, Minneapolis, Minnesota 55455, USA*
[60]*University of Muenster, Wilhelm-Klemm-Street 9, 48149 Muenster, Germany*
[61]*University of Oxford, Keble Road, Oxford OX13RH, United Kingdom*
[62]*University of Science and Technology Liaoning, Anshan 114051, People's Republic of China*
[63]*University of Science and Technology of China, Hefei 230026, People's Republic of China*
[64]*University of South China, Hengyang 421001, People's Republic of China*
[65]*University of the Punjab, Lahore-54590, Pakistan*
[66a]*University of Turin and INFN, University of Turin, I-10125 Turin, Italy*
[66b]*University of Eastern Piedmont, I-15121 Alessandria, Italy*
[66c]*INFN, I-10125 Turin, Italy*
[67]*Uppsala University, Box 516, SE-75120 Uppsala, Sweden*
[68]*Wuhan University, Wuhan 430072, People's Republic of China*
[69]*Xinyang Normal University, Xinyang 464000, People's Republic of China*
[70]*Zhejiang University, Hangzhou 310027, People's Republic of China*
[71]*Zhengzhou University, Zhengzhou 450001, People's Republic of China*

(Received 1 July 2021; accepted 27 September 2021; published 22 October 2021)

The decay $D_s^+ \to \pi^+\pi^+\pi^-\eta$ is observed for the first time, using e^+e^- collision data corresponding to an integrated luminosity of 6.32 fb^{-1}, collected by the BESIII detector at center-of-mass energies between 4.178 and 4.226 GeV. The absolute branching fraction for this decay is measured to be $\mathcal{B}(D_s^+ \to \pi^+\pi^+\pi^-\eta) = (3.12 \pm 0.13_{\rm stat} \pm 0.09_{\rm syst})\%$. The first amplitude analysis of this decay reveals

[a]Also at Bogazici University, 34342 Istanbul, Turkey.
[b]Also at the Moscow Institute of Physics and Technology, Moscow 141700, Russia.
[c]Also at the Novosibirsk State University, Novosibirsk 630090, Russia.
[d]Also at the NRC "Kurchatov Institute," PNPI, 188300 Gatchina, Russia.
[e]Also at Istanbul Arel University, 34295 Istanbul, Turkey.
[f]Also at Goethe University Frankfurt, 60323 Frankfurt am Main, Germany.
[g]Also at Key Laboratory for Particle Physics, Astrophysics and Cosmology, Ministry of Education; Shanghai Key Laboratory for Particle Physics and Cosmology; Institute of Nuclear and Particle Physics, Shanghai 200240, People's Republic of China.
[h]Also at Key Laboratory of Nuclear Physics and Ion-beam Application (MOE) and Institute of Modern Physics, Fudan University, Shanghai 200443, People's Republic of China.
[i]Also at Harvard University, Department of Physics, Cambridge, Massachusetts 02138, USA.
[j]Currently at Institute of Physics and Technology, Peace Avenue 54B, Ulaanbaatar 13330, Mongolia.
[k]Also at State Key Laboratory of Nuclear Physics and Technology, Peking University, Beijing 100871, People's Republic of China.
[l]School of Physics and Electronics, Hunan University, Changsha 410082, China.
[m]Also at Guangdong Provincial Key Laboratory of Nuclear Science, Institute of Quantum Matter, South China Normal University, Guangzhou 510006, China.

the substructures in $D_s^+ \to \pi^+\pi^+\pi^-\eta$ and determines the relative fractions and the phases among these substructures. The dominant intermediate process is $D_s^+ \to a_1(1260)^+\eta, a_1(1260)^+ \to \rho(770)^0\pi^+$ with a branching fraction of $(1.73 \pm 0.14_{\rm stat} \pm 0.08_{\rm syst})\%$. We also observe the W-annihilation process $D_s^+ \to a_0(980)^+\rho(770)^0$, $a_0(980)^+ \to \pi^+\eta$ with a branching fraction of $(0.21 \pm 0.08_{\rm stat} \pm 0.05_{\rm syst})\%$, which is larger than the branching fractions of other measured pure W-annihilation decays by 1 order of magnitude.

DOI: 10.1103/PhysRevD.104.L071101

Since the discovery of the charm quark in 1974, the hadronic decays of charmed mesons have been extensively studied both experimentally and theoretically. However, making precise Standard Model predictions for exclusive weak charm meson decays is rather difficult because the charm quark mass is not heavy enough to allow for a sensible heavy quark expansion, as corrections of higher orders in $1/m_c$ become very important, nor is it light enough for the application of chiral perturbation theory [1]. Studies of hadronic D_s^+ decays provide insight into its decay mechanisms. The Cabibbo-favored (CF) hadronic D_s^+ decays mediated via a $c \to sW, W \to u\bar{d}$ transition, producing states with hidden strangeness ($s\bar{s}$ quarks in η), have relatively large branching fractions (BFs), although some of them have still not been measured. The Particle Data Group (PDG) [2] reports that the missing hadronic decays of D_s^+ with η in the final state contribute a fraction of $(7.1 \pm 3.2)\%$. Among them, the $D_s^+ \to \pi^+\pi^+\pi^-\eta$ decay is expected to have a large BF, but until now it has not been observed.

The topological diagram analysis of the hadronic D_s^+ decays [3] reveals the importance of weak annihilation contributions [4]. The amplitude of the long-distance weak annihilation induced by final-state interactions may be comparable to the tree amplitude [1,4]. The BF of the pure W-annihilation (WA) process with a PP final state, $D_s^+ \to \pi^0\pi^+$, is less than 0.037% [5], and that of the VP final state, $D_s^+ \to \rho(770)^0\pi^+$, is 0.019% [2], while the BF of the WA process with an SP final state, $D_s^+ \to a_0(980)^{+(0)}\pi^{0(+)}, a_0(980)^{+(0)} \to \pi^{+(0)}\eta$, is about 1.46% [6]. Here, V, P, and S denote vector, pseudoscalar, and scalar mesons, respectively. Since the direct production of the $a_0(980)\pi$ system via the $c\bar{s} \to W^+ \to u\bar{d} \to a_0(980)\pi$ transition violates G-parity conservation [7], the WA process $D_s^+ \to a_0^{+(0)}\pi^{0(+)}$ is suppressed. The origin of the abnormally large BF for the SP decay mode is still controversial. Reference [8] argues that the SP decay mode can be produced via internal emission due to which $a_0(980)$ can be dynamically generated from $K\bar{K}$ final-state interactions in coupled channels. Reference [9] claims that $D_s^+ \to a_0(980)^{+(0)}\pi^{0(+)}$ receives the main contribution from $D_s^+ \to \rho(770)^{+(0)}\eta$ through a triangle rescattering process. To date, there have been no theoretical or experimental studies of the WA process with a VS final state. The process $D_s^+ \to a_0(980)^+\rho(770)^0$ can proceed via a WA transition with G-parity conservation. The decay diagram for this decay is shown in Fig. 1. A measurement of this process is critical to distinguish various weak annihilation mechanisms. In addition, the underlying structure of the resonance $a_0(980)^+$ plays an important role in the decay mechanism of the process $D_s^+ \to a_0(980)^+\rho(770)^0$. However, the interpretation of $a_0(980)^+$ is still controversial [2]. Studying the decay $D_s^+ \to a_0(980)^+\rho(770)^0$ can play a key role in understanding the nature of $a_0(980)^+$.

A further motivation to study this decay arises from the tension between theoretical calculations and experimental measurements of the ratio of rates of semileptonic B decays involving leptons from two families. The ratio of the BFs $R(D^*) = \mathcal{B}(B \to D^*\tau\nu)/\mathcal{B}(B \to D^*l\nu)$ ($l = e, \mu$) averaged by HFLAV is $0.295 \pm 0.011 \pm 0.008$. It differs from the Standard Model prediction of 0.258 ± 0.005 by 2.6 standard deviations [10]. This suggests violation of the lepton flavor universality. However, experimental measurements at LHCb have a large systematic uncertainty from the limited knowledge of the inclusive $D_s^+ \to \pi^+\pi^+\pi^-X$ decay [11]. A precise measurement of the decay $D_s^+ \to \pi^+\pi^+\pi^-\eta$ may provide useful input to this problem.

This paper reports the first observation of the $D_s^+ \to \pi^+\pi^+\pi^-\eta$ decay, along with an amplitude analysis and a BF measurement of this decay. This analysis uses e^+e^- collision data samples corresponding to an integrated luminosity of 6.32 fb^{-1} collected at the center-of-mass energies ($E_{\rm cm}$) between 4.178 and 4.226 GeV. Throughout this paper, charged-conjugate modes and exchange symmetry of two identical π^+ are always implied.

The BESIII detector and the upgraded multigap resistive plate chambers used in the time-of-flight systems are described in Refs. [12,13], respectively. Simulated data

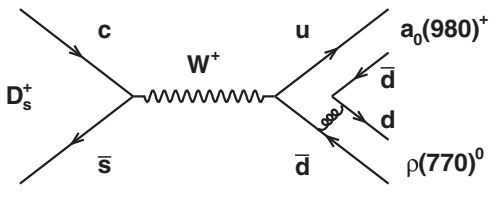

FIG. 1. $D_s^+ \to \pi^+\pi^+\pi^-\eta$ WA-topology diagrams, where the gluon lines can be connected with the quark lines in all possible configurations.

samples produced with a Geant4-based [14] Monte Carlo (MC) program, which includes the geometric description of the BESIII detector and the detector response, are used to determine detection efficiencies and to estimate backgrounds. The simulation models the beam energy spread and initial-state radiation (ISR) in the e^+e^- annihilations with the generator KKMC [15]. The inclusive MC sample includes the production of open charm processes modeled with CONEXC [16], the ISR production of vector charmonium(-like) states, and the continuum processes incorporated in KKMC [15]. The known decay modes are modeled with EVTGEN [17] using BFs taken from the PDG [2], and the remaining unknown charmonium decays are modeled with LUNDCHARM [18]. Final-state radiation (FSR) from charged final-state particles is incorporated using PHOTOS [19].

We employ the double-tag (DT) technique [20] to select $D_s^+ \to \pi^+\pi^+\pi^-\eta$ decays in $e^+e^- \to D_s^{*\pm}D_s^{\mp}, D_s^{*\pm} \to \gamma D_s^{\pm}$ events. The single-tag (ST) D_s^- candidates are reconstructed from eight hadronic decay modes (tag side): $D_s^- \to K_S^0K^-$, $K^+K^-\pi^-$, $K_S^0K^-\pi^0$, $K^-K^+\pi^-\pi^0$, $K_S^0K^-\pi^+\pi^-$, $K_S^0K^+\pi^-\pi^-$, $\pi^-\eta'$, and $K^-\pi^+\pi^-$. These tag modes are combined to perform an amplitude analysis. A DT candidate is selected by reconstructing the $D_s^+ \to \pi^+\pi^+\pi^-\eta$ decay (signal side) from the remaining particles that are not used in the ST reconstruction. Here, the K_S^0, π^0, η, and η' mesons are reconstructed from $K_S^0 \to \pi^+\pi^-$, $\pi^0 \to \gamma\gamma$, $\eta \to \gamma\gamma$, and $\eta' \to \pi^+\pi^-\eta$ decays, respectively. The selection criteria for charged and neutral particle candidates are identical to those used in Ref. [21]. For the decay mode $D_s^- \to K^-\pi^+\pi^-$, we exclude the dipion mass range $[0.487, 0.511]$ GeV/c^2 to avoid overlap with the $D_s^- \to K_S^0K^-$ mode.

The invariant mass of the tag (signal) $D_s^{-(+)}$ candidate $M_{\rm tag}$ ($M_{\rm sig}$) is required to be within the range $[1.87, 2.06]$ GeV/c^2. We calculate the recoiling mass $M_{\rm rec} = \{[E_{\rm cm} - (\vec{p}^{\,2}_{D_s^-} + m^2_{D_s^-})^{1/2}]^2 - |\vec{p}_{D_s^-}|^2\}^{1/2}$ in the e^+e^- center-of-mass system, where $\vec{p}_{D_s^-}$ is the momentum of the reconstructed D_s^- and $m_{D_s^-}$ is the known mass of the D_s^- meson [2]. The value of $M_{\rm rec}$ is required to be in the range $[2.05, 2.18]$ GeV/c^2 for the data sample collected at 4.178 GeV to suppress the non-$D_s^{*\pm}D_s^{\mp}$ events. The $M_{\rm rec}$ ranges for the other data samples are the same as those in Ref. [22].

A seven-constraint kinematic fit is applied to the $e^+e^- \to D_s^{*\pm}D_s^{\mp} \to \gamma D_s^+D_s^-$ candidates, where D_s^- decays to one of the tag modes and D_s^+ decays to the signal mode. In addition to the constraints of four-momentum conservation in the e^+e^- center-of-mass system, the invariant masses of η, tag D_s^-, and D_s^{*+} candidates are constrained to their individual PDG values [2]. If there are multiple candidates (in ≈15% of the selected events) in an event, the one with the minimum χ^2 of the seven-constraint kinematic fit is accepted.

To suppress the background from $D_s^+ \to K_S^0\pi^+\eta$ decays, a secondary vertex fit [23] is performed on the $\pi^+\pi^-$ pair. If its invariant mass is in the range $[0.487, 0.511]$ GeV/c^2 and the flight distance between the interaction point (IP) [23] and the decay point is 2 times greater than its uncertainty, we reject these candidates. To suppress the background from the decay $D_s^+ \to \pi^+\eta'$ with $\eta' \to \pi^+\pi^-\eta$, we reject candidates with $M_{\pi^+\pi^-\eta} < 1$ GeV/c^2. To suppress the background where individual photons from random π^0's feed into the $\eta \to \gamma\gamma$ reconstruction, we define two invariant masses $M(\gamma_\eta\gamma_{\pi^0})$ and $M(\gamma_\eta\gamma_{\rm other})$, where γ_η, γ_{π^0}, and $\gamma_{\rm other}$ denote the photon of η from the signal side, the photon of π^0 from the tag side, and the other photons including the transition photon from $D_s^{*+(-)}$, respectively. We reject events with $M(\gamma_\eta\gamma_{\pi^0})$ or $M(\gamma_\eta\gamma_{\rm other})$ in the range $[0.115, 0.150]$ GeV/c^2.

We further reduce the background by using a gradient-boosted decision tree (BDT) implemented in the TMVA software package [24]. The BDT takes four discriminating variables as inputs: the recoiling mass of D_s^*, the momentum of the lower-energy photon from η, the invariant mass of the two photons used to reconstruct η, and the energy of the transition photon from D_s^*. We place a requirement on the output of the BDT to ensure the samples have a purity greater than 85%: $(87.0 \pm 3.8)\%$, $(85.6 \pm 4.9)\%$, and $(89.2 \pm 9.2)\%$ at $E_{\rm cm} = 4.178$, 4.189–4.219, and 4.226 GeV, respectively.

An unbinned maximum likelihood method is adopted in the amplitude analysis of the $D_s^+ \to \pi^+\pi^+\pi^-\eta$ decay. The likelihood function is constructed with a probability density function (PDF) in which the momenta of the four final-state particles are used as inputs. The total likelihood is the product of the likelihoods for all data samples. The total amplitude is modeled as a coherent sum over all intermediate processes $M(p_j) = \sum \rho_n e^{i\phi_n} A_n(p_j)$, where $\rho_n e^{i\phi_n}$ is the coefficient of the nth amplitude with magnitude ρ_n and phase ϕ_n. The nth amplitude $A_n(p_j)$ is given by $A_n = P_n^1 P_n^2 S_n F_n^1 F_n^2 F_n^3$, where the indices 1, 2, and 3 correspond to the two subsequent intermediate resonances and the D_s^+ meson, F_n^i is the Blatt-Weisskopf barrier factor [25,26], and P_n^i is the propagator of the intermediate resonance. The function S_n describes angular-momentum conservation in the decay and is constructed using the covariant tensor formalism [26]. The relativistic Breit-Wigner (RBW) [27] function is used to describe the propagator for the resonances $\eta(1405)$, $f_1(1420)$, and $a_1(1260)$. The resonance $\rho(770)^+$ is parametrized by the Gounaris-Sakurai [28] line shape, the resonances $a_0(980)$ and $f_0(980)$ are parametrized by a coupled Flatté formula, and the parameters are fixed to the values given in Refs. [29] and [30], respectively. We use the same parametrization to describe $f_0(500)$ as Ref. [31]. The masses and widths of the intermediate resonances, except for $a_0(980)$, $f_0(980)$, and $f_0(500)$, are taken from Ref. [2].

The background PDF $B(p_j)$ is constructed from inclusive MC samples by using a multidimensional kernel density estimator [32] with five independent Lorentz invariant variables ($M_{\pi^+\pi^+}$, $M_{\pi^+\pi^-}$, $M_{\pi^+\eta}$, $M_{\pi^-\eta}$, and $M_{\pi^+\pi^-\eta}$). As a consequence, the combined PDF can be written as

$$\epsilon R_4\left[f_s\frac{|M(p_j)|^2}{\int\epsilon|M(p_j)|^2R_4dp_j}+(1-f_s)\frac{B_\epsilon(p_j)}{\int\epsilon B_\epsilon(p_j)R_4dp_j}\right],$$

where ϵ is the acceptance function determined with phase-space (PHSP) MC samples generated with a uniform distribution of the $D_s^+\to\pi^+\pi^+\pi^-\eta$ decay over PHSP, B_ϵ is B/ϵ, and R_4dp_j is the element of four-body PHSP. The normalization integral in the denominator is determined by a MC technique as described in Ref. [33].

In the initial amplitude fit, we include a few obvious components. Then, further amplitudes are added one at a time to the fit, and the statistical significance of the new amplitude is calculated with the change of the log-likelihood, after taking the change of the degrees of freedom into account. Only amplitudes with significance larger than 5σ are chosen for the optimal set. The dominant CF amplitude for this final state is $D_s^+\to a_1(1260)^+\eta, a_1(1260)\to[\rho(770)^0\pi^+]_S$, where the subscript S means that the angular momentum of the $\rho^0\pi^+$ combination is zero (S-wave). Thus, we choose this amplitude as the reference, and its phase is fixed to 0. The $D_s^+\to a_0(980)^+\rho(770)^0$, $a_0(980)^+\to\pi^+\eta$ decay is observed with a significance larger than 7σ. We also consider some possible amplitudes involving the resonances $f_0(500)$, $f_0(980)$, $f_1(1285)$, $\eta(1295)$, $\eta(1405)$, $\eta(1475)$, $f_1(1420)$, $f_1(1510)$, and $\pi(1300)$, as well as nonresonant components. Moreover, charge conjugation for $D_s^+\to\eta(1405)(f_1(1420))\pi^+$ with $\eta(1405)(f_1(1420))\to a_0(980)^+\pi^-$ and $\eta(1405)(f_1(1420))\to a_0(980)^-\pi^+$ requires their magnitudes and phases to be the same. Finally, eleven amplitudes are retained in the nominal fit, as listed in Table I. The mass projections of the fit are shown in Fig. 2. For the nth component, its contribution relative to the total BF is quantified by the fit fraction (FF) defined by $\mathrm{FF}_n=\int|\rho_nA_n(p_j)|^2R_4dp_j/\int|M|^2R_4dp_j$. The final amplitudes, their phases, and FFs are listed in Table I. The sum of the FFs of all the components is $(95.0\pm4.9)\%$. A χ^2 value is calculated to quantify the quality of the fit, as defined in Ref. [33]. The goodness of fit is $\chi^2/\mathrm{NDOF}=153.2/133=1.15$ and the p-value is 11.1%. In addition, 300 sets of signal MC samples with the same size as the data samples are generated to validate the fit performance, as described in Ref. [21]. No significant bias is found in our fit.

We determine the systematic uncertainties by taking the differences between the values of ϕ_n and FF_n found by the nominal fit and those found from fit variations. The masses and widths of the intermediate states are varied by $\pm1\sigma$ [2]. The masses and coupling constants of $a_0(980)$ and $f_0(980)$ are varied within the uncertainties reported in Refs. [29] and [30], respectively. The barrier radii for D_s^+ and the other intermediate states are varied by ±1 GeV^{-1}. The uncertainties related to line shape are estimated by using an alternative RBW function for $f_0(500)$ with mass and width fixed to 526 MeV/c^2 and 535 MeV [34]. The uncertainties from detector effects are investigated with the same method as described in Ref. [21]. The uncertainty related to the background is estimated by varying the background yield within statistical uncertainty and constructing the background PDF with the other five independent variables. The total uncertainties are obtained by adding all the contributions in quadrature and are listed in Table I.

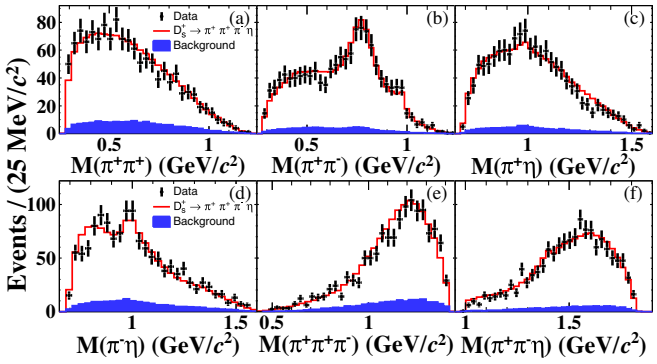

FIG. 2. (a) $M_{\pi^+\pi^+}$, (b) $M_{\pi^+\pi^-}$, (c) $M_{\pi^+\eta}$, (d) $M_{\pi^-\eta}$, (e) $M_{\pi^+\pi^+\pi^-}$, and (f) $M_{\pi^+\pi^-\eta}$ projections for data with the best fit superimposed. The dots with error bars, the red histograms, and the blue histograms are data from all samples, the total fit, and the background contribution estimated with inclusive MC samples, respectively. Since the two π^+'s in the final state are identical particles, they have a symmetric wave function in some states. The projections of $M_{\pi^+\pi^-}$, $M_{\pi^+\pi^-\eta}$ and $M_{\pi^+\eta}$ are added for the two π^+'s.

Further, we measure the BF of $D_s^+\to\pi^+\pi^+\pi^-\eta$ with the DT technique. To improve the statistical precision, the DT candidates are selected without reconstructing the transition

TABLE I. Phases and FFs for various intermediate processes. The first and the second uncertainties are statistical and systematic, respectively.

Amplitude	Phase	FF (%)
$a_1(1260)^+(\rho(770)^0\pi^+)\eta$	0.0 (fixed)	$55.4\pm3.9\pm2.0$
$a_1(1260)^+(f_0(500)\pi^+)\eta$	$5.0\pm0.1\pm0.1$	$8.1\pm1.9\pm2.1$
$a_0(980)^+\rho(770)^0$	$2.5\pm0.1\pm0.1$	$6.7\pm2.5\pm1.5$
$\eta(1405)(a_0(980)^-\pi^+)\pi^+$	$0.2\pm0.2\pm0.1$	$0.7\pm0.2\pm0.1$
$\eta(1405)(a_0(980)^+\pi^-)\pi^+$	$0.2\pm0.2\pm0.1$	$0.7\pm0.2\pm0.1$
$f_1(1420)(a_0(980)^-\pi^+)\pi^+$	$4.3\pm0.2\pm0.4$	$1.9\pm0.5\pm0.3$
$f_1(1420)(a_0(980)^+\pi^-)\pi^+$	$4.3\pm0.2\pm0.4$	$1.7\pm0.5\pm0.3$
$[a_0(980)^-\pi^+]_S\pi^+$	$0.1\pm0.2\pm0.2$	$5.1\pm1.2\pm0.9$
$[a_0(980)^+\pi^-]_S\pi^+$	$0.1\pm0.2\pm0.2$	$3.4\pm0.8\pm0.6$
$[f_0(980)\eta]_S\pi^+$	$1.4\pm0.2\pm0.3$	$6.2\pm1.7\pm0.9$
$[f_0(500)\eta]_S\pi^+$	$2.5\pm0.2\pm0.3$	$12.7\pm2.6\pm2.0$

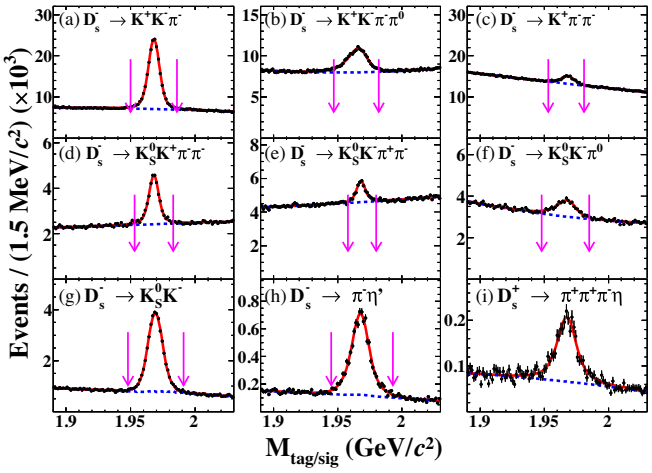

FIG. 3. Fits to (a)–(h) the $M_{\rm tag}$ distributions of the ST candidates and (i) the $M_{\rm sig}$ distribution of the signal candidates. The dots with error bars are data from all samples. The red solid lines are the fits. The dashed blue lines are the fitted background shapes. The pair of pink arrows mark the chosen signal region. In the plots for $D_s^- \to K_S^0K^-$ and $D_s^- \to \pi^-\eta'$ decays, the blue dashed lines include contributions from $D^- \to K_S^0\pi^-$ and $D_s^- \to \pi^+\pi^-\pi^-\eta$ backgrounds, respectively.

photon from D_s^* and without the BDT requirement. We use the same eight tag modes as used in the amplitude analysis. For each tag mode, if there are multiple tag D_s^- candidates, the one with $M_{\rm rec}$ closest to the known mass of D_s^* [2] is retained. For each tag mode, a DT candidate with the average mass $(M_{\rm sig}+M_{\rm tag})/2$ closest to the known mass of D_s [2] is retained. The ST yield ($Y_{\rm tag}$) and DT yield ($Y_{\rm sig}$) in data are determined from fits to the $M_{\rm tag}$ and $M_{\rm sig}$ distributions, respectively, as shown in Fig. 3. The signal shape is modeled with the MC-simulated shape convolved with a Gaussian function, and the background is parametrized as a second-order Chebyshev function.

These fits result in a total ST yield of $Y_{\rm tag} = 479{,}093 \pm 1952$ and a signal yield of $Y_{\rm sig} = 2139 \pm 78$ events. An updated inclusive MC sample based on our amplitude analysis results is used to determine the ST efficiencies ($\epsilon_{\rm ST}^i$) and DT efficiencies ($\epsilon_{\rm DT}^i$). Inserting these numbers in $\mathcal{B}(D_s^+ \to \pi^+\pi^+\pi^-\eta) = Y_{\rm sig}/(\mathcal{B}(\eta\to\gamma\gamma)\times\Sigma_{i,\alpha}Y_{\rm tag}^{i,\alpha}\epsilon_{\rm DT}^{i,\alpha}/\epsilon_{\rm ST}^{i,\alpha})$, where i denotes the ith tag mode and α denotes the αth center-of-mass energy point, we obtain $\mathcal{B}(D_s^+ \to \pi^+\pi^+\pi^-\eta) = (3.12 \pm 0.13)\%$, where the uncertainty is statistical only.

The systematic uncertainties for the BF measurement are described next. The uncertainty of the signal yield and total ST yield is assigned to be 1.4% by examining the changes of the fit yields when varying the signal and background shapes. The $\pi^\pm$ tracking (PID) efficiencies are studied using samples of $e^+e^- \to K^+K^-\pi^+\pi^-$ ($e^+e^- \to K^+K^-\pi^+\pi^-$ and $\pi^+\pi^-\pi^+\pi^-$) events. The corresponding systematic uncertainties are estimated as 0.3% (0.4%). The uncertainty due to the η reconstruction efficiency is 2.0% [6]. The uncertainty from the amplitude model is estimated to be 0.4%, which is the change of signal efficiency when the parameters are varied according to the covariance matrix in the nominal amplitude fit. The uncertainty due to MC simulation sample size is 0.3%, and that from the BF of $\mathcal{B}(\eta\to\gamma\gamma)$ is 0.5% [2]. Adding these uncertainties in quadrature gives a total systematic uncertainty of 2.9%.

In summary, using e^+e^- collision data equivalent to an integrated luminosity of 6.32 fb^{-1} recorded with the BESIII detector at $E_{\rm cm} = 4.178$–4.226 GeV, we observe the $D_s^+ \to \pi^+\pi^+\pi^-\eta$ decay for the first time. The absolute BF of this decay is measured to be $\mathcal{B}(D_s^+ \to \pi^+\pi^+\pi^-\eta) = (3.12 \pm 0.13_{\rm stat} \pm 0.09_{\rm syst})\%$. The first amplitude analysis of this decay is also performed. The obtained intermediate processes, phases, and FFs are summarized in Table I. The BFs for the intermediate processes are calculated with $\mathcal{B}_n = {\rm FF}_n \times \mathcal{B}(D_s^+ \to \pi^+\pi^+\pi^-\eta)$. The $D_s^+ \to a_1(1260)^+\eta, a_1(1260)^+ \to \rho(770)^0\pi^+$ decay is dominant with a BF of $(1.73 \pm 0.14_{\rm stat} \pm 0.08_{\rm syst})\%$. Our results offer critical input for estimating the $D_s^+ \to \pi^+\pi^+\pi^-X$ background contribution in tests of the lepton flavor universality with semileptonic B decays. Assuming that $\mathcal{B}(a_1(1260)^+ \to \rho(770)^+\pi^0) = \mathcal{B}(a_1(1260)^+ \to \rho(770)^0\pi^+)$, the BF of $D_s^+ \to \pi^+\pi^0\pi^0\eta$ decay is expected to be comparable to the one of $D_s^+ \to \pi^+\pi^+\pi^-\eta$. In this case, the missing inclusive hadronic η decay fraction of D_s^+ is reduced to $(2.3 \pm 3.2)\%$, thereby indicating that there is not much room for unobserved exclusive $D_s^+ \to \eta X$ decays. Furthermore, we observe the WA decay $D_s^+ \to a_0(980)^+\rho(770)^0, a_0(980)^+ \to \pi^+\eta$ with BF of $(0.21 \pm 0.08_{\rm stat} \pm 0.05_{\rm syst})\%$. This BF and the one of the decay $D_s^+ \to a_0(980)^+\pi^0$ obtained in Ref. [6] are both larger than those of the pure WA processes $D_s^+ \to \rho(770)^0\pi^+$ and $D_s^+ \to \pi^0\pi^+$ by 1 order of magnitude. These measurements indicate that long-distance weak annihilation may play an essential role, and they provide a good opportunity to study the final-state rescattering in the WA process [1,8,9].

The BESIII Collaboration thanks the staff of BEPCII and the IHEP computing center for their strong support. This work is supported in part by the National Key Research and Development Program of China under Contracts No. 2020YFA0406400 and No. 2020YFA0406300; National Natural Science Foundation of China (NSFC) under Contracts No. 11625523, No. 11635010, No. 11735014, No. 11822506, No. 11835012, No. 11935015, No. 11935016, No. 11935018, and No. 11961141012; the Chinese Academy of Sciences (CAS) Large-Scale Scientific Facility Program; Joint Large-Scale Scientific Facility Funds of the NSFC and CAS under Contracts No. U1732263, No. U1832107, and No. U1832207; CAS Key Research Program of Frontier Sciences under Contract No. QYZDJ-SSW-SLH040; 100 Talents Program of CAS; INPAC and Shanghai Key

Laboratory for Particle Physics and Cosmology; ERC under Contract No. 758462; European Union Horizon 2020 research and innovation programme under Contract No. Marie Sklodowska-Curie Grant Agreement No. 894790; German Research Foundation DFG under Contract No. 443159800, Collaborative Research Center CRC 1044, FOR 2359, GRK 214; Istituto Nazionale di Fisica Nucleare, Italy; Ministry of Development of Turkey under Contract No. DPT2006K-120470; National Science and Technology fund; Olle Engkvist Foundation under Contract No. 200-0605; STFC (United Kingdom); the Knut and Alice Wallenberg Foundation (Sweden) under Contract No. 2016.0157; the Royal Society, UK under Contracts No. DH140054 and No. DH160214; the Swedish Research Council; and the U.S. Department of Energy under Contracts No. DE-FG02-05ER41374 and No. DE-SC-0012069.

[1] H. Y. Cheng and C. W. Chiang, Phys. Rev. D **81**, 074021 (2010).
[2] P. A. Zyla *et al.* (Particle Data Group Collaboration), Prog. Theor. Exp. Phys. **2020**, 083C01 (2020) .
[3] L. L. Chau and H. Y. Cheng, Phys. Rev. D **36**, 137 (1987).
[4] J. L. Rosner, Phys. Rev. D **60**, 114026 (1999).
[5] H. Mendez *et al.* (CLEO Collaboration), Phys. Rev. D **81**, 052013 (2010).
[6] M. Ablikim *et al.* (BESIII Collaboration), Phys. Rev. Lett. **123**, 112001 (2019).
[7] N. N. Achasov and G. N. Shestakov, Phys. Rev. D **96**, 036013 (2017).
[8] R. Molina, Ju-Jun Xie, Wei-Hong Liang, Li-Sheng Geng, and Eulogio Oset, Phys. Lett. B **803**, 135279 (2020).
[9] Y. K. Hsiao, Yao Yu, and Bai-Cian Ke, Eur. Phys. J. C **80**, 895 (2020).
[10] Y. Amhis *et al.* (Heavy Flavor Averaging Group Collaboration), Eur. Phys. J. C **77**, 895 (2017); updated results available at https://hflav-eos.web.cern.ch/hflav-eos/semi/spring19/html/RDsDsstar/RDRDs.html.
[11] R. Aaij *et al.* (LHCb Collaboration), Phys. Rev. Lett. **120**, 171802 (2018).
[12] M. Ablikim *et al.* (BESIII Collaboration), Nucl. Instrum. Methods Phys. Res., Sect. A **614**, 345 (2010).
[13] X. Wang *et al.*, J. Instrum. **11**, C08009 (2016).
[14] S. Agostinelli *et al.* (GEANT4 Collaboration), Nucl. Instrum. Methods Phys. Res., Sect. A **506**, 250 (2003).
[15] S. Jadach, B. F. L. Ward, and Z. Was, Phys. Rev. D **63**, 113009 (2001).
[16] R. G. Ping, Chin. Phys. C **38**, 083001 (2014).
[17] D. J. Lange, Nucl. Instrum. Methods Phys. Res., Sect. A **462**, 152 (2001); R. G. Ping, Chin. Phys. C **32**, 243 (2008).
[18] J. C. Chen, G. S. Huang, X. R. Qi, D. H. Zhang, and Y. S. Zhu, Phys. Rev. D **62**, 034003 (2000); R. L. Yang, R. G. Ping, and H. Chen, Chin. Phys. Lett. **31**, 061301 (2014).
[19] P. Golonka and Z. Was, Eur. Phys. J. C **45**, 97 (2006).
[20] R. M. Baltrusaitis *et al.* (Mark III Collaboration), Phys. Rev. Lett. **56**, 2140 (1986).
[21] M. Ablikim *et al.* (BESIII Collaboration), Phys. Rev. D **104**, 012016 (2021).
[22] M. Ablikim *et al.* (BESIII Collaboration), Phys. Rev. D **103**, 092006 (2021).
[23] M. Xu *et al.*, Chin. Phys. C **33**, 428 (2009).
[24] A. Hocker *et al.*, Proc. Sci. ACAT2007 (**2007**) 040.
[25] J. M. Blatt and V. F. Weisskopf, *Theoretical Nuclear Physics* (John Wiley & Sons, New York, 1973).
[26] B. S. Zou and D. V. Bugg, Eur. Phys. J. A **16**, 537 (2003).
[27] J. D. Jackson, Nuovo Cimento **34**, 1644 (1964).
[28] G. J. Gounaris and J. J. Sakurai, Phys. Rev. Lett. **21**, 244 (1968).
[29] M. Ablikim *et al.* (BESIII Collaboration), Phys. Rev. D **95**, 032002 (2017).
[30] M. Ablikim *et al.* (BESIII Collaboration), Phys. Lett. B **607**, 243 (2005).
[31] D. V. Bugg, A. V. Sarantsev, and B. S. Zou, Nucl. Phys. **B471**, 59 (1996).
[32] K. S. Cranmer, Comput. Phys. Commun. **136**, 198 (2001).
[33] M. Artuso *et al.* (CLEO Collaboration), Phys. Rev. D **85**, 122002 (2012).
[34] M. Ablikim *et al.* (BESII Collaboration), Phys. Lett. B **598**, 149 (2004).